

Nature and Origin of a Massive Sulfide Occurrence in the Karrat Group: Evidence for Paleoproterozoic VMS Mineralization in Central West Greenland

Y. M. DeWolfe,^{1,†} J. Kolb,³ E. V. Sorensen,² D. Rosa,² and P. Guarnieri²

¹*Department of Earth and Environmental Sciences, Mount Royal University, Calgary, Alberta T3E 6K6, Canada*

²*Geological Survey of Denmark and Greenland, Copenhagen 1350, Denmark*

³*Karlsruhe Institute of Technology, Institute of Applied Geosciences, Karlsruhe 7613, Germany*

Abstract

Mafic volcanic rocks of the Kangilleq Formation of the Paleoproterozoic Karrat Group host volcanogenic massive sulfide (VMS) mineralization in the area of central Kangiasap Kuua, central West Greenland. The mafic volcanic rocks display evidence of subaqueous, effusive eruption and redeposition by mass debris flows generated along fault scarps on the sea floor. A zone of semiconformable quartz alteration and disconformable chlorite alteration within hydrothermal breccias and mafic tuff breccias near the top of the volcanic sequence is interpreted to reflect a synvolcanic hydrothermal system. Conformable, massive to semimassive, and discordant, stringer-style sulfide mineralization is hosted within the quartz- and chlorite-altered volcanic rocks. The massive to semimassive sulfide mineralization is ~10 m thick and crops out along strike for ~2,000 m. The stringer zone is ≤10 m thick with individual sulfide stringers ranging in width from 5 to 90 cm. All sulfide zones are dominated by coarse pyrrhotite and pyrite, with trace amounts of sphalerite and chalcopyrite.

The pillow lavas are subalkaline with geochemical characteristics typical of modern transitional to tholeiitic mid-ocean ridge or back-arc basin basalt. Trace element and Nd isotope data suggest that these lavas erupted in an epicratonic, back-arc basin. Characteristics of the host rocks indicate a period of localized rifting, volcanism, and VMS formation during genesis of the Karrat Group, which is dominated by siliciclastic rocks.

Introduction

Volcanogenic massive sulfide (VMS) deposits are an important source for base and precious metals globally (Lydon, 1984; Ohmoto, 1996; Franklin et al., 2005; Hannington, 2014). Although Phanerozoic rocks contain 72% of the world's VMS tonnage, the Proterozoic is the next most prolific eon, accounting for ~20% of global VMS tonnage (Franklin et al., 2005). Whereas ore-forming processes and environments of VMS deposits are well understood (Allen et al., 2002, 2011; Franklin et al., 2005; Galley et al., 2007), discovering these typically small but high-grade deposits remains a significant challenge, especially in strongly deformed and metamorphosed rocks. Exploration for Precambrian VMS deposits is further complicated in the northern hemisphere by the fact that these rocks are commonly covered by glacial deposits or are deeply weathered. For these reasons, and despite the occurrence of prospective Precambrian volcanic terranes, no significant VMS mineralization has been documented in Greenland, Precambrian or younger, although there are several known stratiform semi- to massive sulfide occurrences, and two are thought to be potentially VMS. In the Archean Naternaq belt south of Disko Bugt, the Naternaq/Lersletten Cu-Zn deposit (Fig. 1) comprises sulfide-hosting quartz mineralization hosted by amphibolite or marble and is speculated to have either VMS or sedimentary-exhalative (SEDEX) affinities (Østergaard et al., 2002; Garde and Hollis, 2010; Kolb et al., 2016). In the Paleoproterozoic Karrat Group, massive sulfide mineralization spatially associated with metamorphosed chert and hydrothermal alteration zones south of

Inngia Isbrae (Fig. 1) is thought to probably represent a metamorphosed volcanic-hosted massive sulfide (VHMS) system (Kolb et al., 2016).

The focus of this study is a ~100-m-thick sequence of mafic volcanic rocks of the Kangilleq Formation that occurs in the N-S-oriented central Kangiasap Kuua (Fig. 1). Massive and stringer-style sulfide mineralization in the central Kangiasap Kuua within the Paleoproterozoic Karrat Group of central West Greenland occurs in outcrop at ca. 71° N, 54° E (Fig. 1). Sulfide concentrations occur at the top of a sequence of metamorphosed pillow basalt and associated mafic volcanoclastic rocks of the Kangilleq Formation and are overlain by metasedimentary rocks of the Nūkavsak Formation. This paper details not only the sulfide mineralization but also the stratigraphy, lithofacies, and hydrothermal alteration of the host rocks, including whole-rock geochemistry and Nd isotope data, and provides the first significant, multimethod documentation of VMS mineralization in Greenland.

The Kangilleq Formation and the VMS mineralization within it represent an integral part of the hydrothermal, volcanic, and tectonic history of the Karrat Group and have direct implications in elucidating epicratonic rift processes and related hydrothermal activity that controlled VMS formation.

Regional Geology

The Paleoproterozoic Karrat Group is a siliciclastic-carbonate-volcanic rock succession that was deposited unconformably on Archean crystalline basement rocks (Henderson and Pulvertaft, 1987) assigned to the Rae craton (Connelly et al., 2006; Dawes, 2006; St-Onge et al., 2009; Thrane, 2021). All of the Karrat Group rocks are metamorphosed, but for clarity are described by their protoliths herein.

[†]Corresponding author: e-mail, mdewolfe@mtroyal.ca

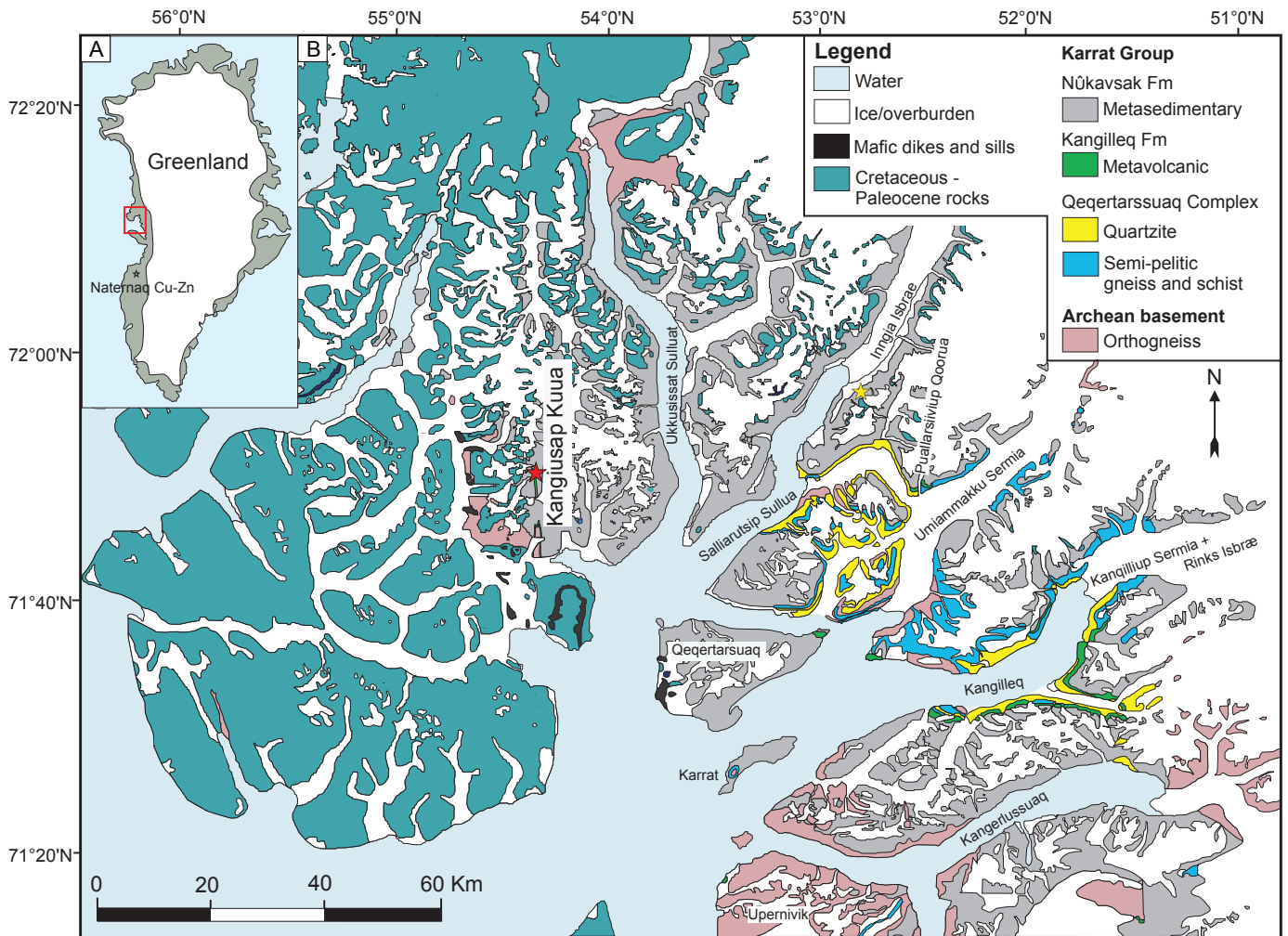


Fig. 1. Geologic map of the Kangilleq area (after Escher, 1980). A. Red box shows the location of study area in central West Greenland and area of main map in this figure; black star shows location of Naternaq Cu-Zn mineralization in the Disko Bugt area. B. Red star marks the location of massive sulfide mineralization in the central Kanguasap Kuua. Yellow star marks the location of massive sulfide associated with metamorphosed chert and hydrothermal alteration zones, but within sedimentary rocks of the Nûkavsak Formation.

The Qeqertarsuaq Formation, previously considered as the lower part of the Karrat Group, is now separated from it and renamed the Qeqertarsuaq Complex (Guarnieri et al., 2022a). The Karrat Group was introduced by Henderson and Pulvertaft (1967, 1987) and recently revised by Guarnieri et al. (2022a-c) to consist of four lithostratigraphic units: the Qarsukassak, Mârmorilik, Kangilleq, and Nûkavsak Formations. The lower part of the Karrat Group is represented by the siliclastic Qarsukassak Formation (Guarnieri et al., 2016) and a marine carbonate platform named the Mârmorilik Formation (Garde and Pulvertaft, 1976). The upper part of the group is represented by volcanic rocks of the Kangilleq Formation and siltstone and sandstone of the Nûkavsak Formation. Discrete, thin (<20-m) mafic units also occur in the Nûkavsak Formation. U-Pb data from detrital zircons reveal a maximum depositional age of ca. 2000 Ma for the Qarsukassak Formation and ca. 1915 Ma for the pelite intercalated with dolomitic marble of the Mârmorilik Formation (Guarnieri et al., 2022a, b). The Nûkavsak Formation has a maximum depositional age of 1953 ± 31 Ma (Sanborn-Barrie et al., 2017).

The Kangilleq Formation comprises volcanic rocks of the Karrat Group (Rosa et al. 2017, 2018). This formation is predominantly basalt and is best exposed in the Kangilleq and Puallarsiivup Qoorua areas (Fig. 1). Although the rocks have undergone greenschist-facies metamorphism conditions, primary volcanic textures such as pillows, scoria, autoclastic breccias, and hyaloclastite are well preserved. Occurrences of pillow lavas and hyaloclastite are unequivocal evidence of eruption in a subaqueous environment (e.g., Dimroth et al., 1978; Dimroth and Yamagishi, 1987).

Methodology

Mapping at 1:200 combined with petrographic observations are used to determine volcanic lithofacies, including modes of eruption or deposition. Volcanic rocks of the Kangilleq Formation are well exposed along a ridge in the central Kanguasap Kuua, and because of the relatively steep erosional valley and dip of the units, exposure of the stratigraphy allows for recognition of the discontinuous nature and interstratification of volcanoclastic units and lava flows and pro-

vides a cross section through the volcanic and hydrothermal system.

Field mapping

A series of stratigraphic sections were completed ~50 to 150 m along strike from each other at a scale of 1:200 from the bottom of the valley, where exposure ends in overburden, to the top of the ridge, ~20 m into the hanging wall of the mineralization (Figs. 2, 3). Each lithofacies was described in terms of primary textures, mineralogy, and alteration. These sections and other field observations were used to create the map shown in Figure 2.

Petrology

Detailed transmitted-light petrography was completed on six samples representing all major lithofacies in the stratigraphy. Reflected-light microscopy was done on four samples of massive to stringer to disseminated sulfide mineralization. Imaging and semiquantitative mineral chemistry was acquired by electron microprobe analyses at the University of Calgary, using a JEOL JXA-8200 electron microprobe that utilizes an 8-channel Thermo Scientific energy dispersive spectrometer (EDS).

Whole-rock geochemistry

Four samples from the Kangilleq Formation in the central Kangiusap Kuua, collected during the 2016 field season, were prepared and analyzed at Activation Laboratories (Actlabs) in Ancaster, Ontario, Canada. Samples were prepared using a steel jaw crusher and pulverized using a steel (mild) mill. Samples were fused using a lithium metaborate/tetraborate fusion, and the resultant molten bead was rapidly digested in weak nitric acid solution and analyzed by inductively coupled plasma-optical emission spectroscopy (ICP-OES; major oxides) and inductively coupled plasma-mass spectrometry (ICP-MS; trace elements). Replicate analyses of samples and standards yielded relative standard deviations (% RSD) of <10% for ICP-MS and <18% for ICP-OES, and relative differences (%RD) of <8% for both ICP-MS and ICP-OES determinations.

One basalt sample was analyzed for whole-rock neodymium (Nd) isotopes at the Earth Resources Research and Analysis Facility, Department of Earth Sciences, Memorial University of Newfoundland, using thermal ionization mass spectrometry (TIMS), following the methods of Pollock et al. (2015). Initial $^{143}\text{Nd}/^{144}\text{Nd}$ ratios and ϵ_{Nd} were calculated at 1.9 Ga, based on the approximate maximum age of the Nukavsak Formation (Sanborn-Barrie et al., 2017).

Five massive to semimassive sulfide samples were analyzed at Actlabs, using the peroxide “total” fusion ore-assay method (8-peroxide fusion ICPMS/ICP). Samples were fused with sodium peroxide and underwent an acid dissolution. Samples were then analyzed by ICP-MS.

Lithofacies

In the lithofacies descriptions the term volcanoclastic refers to “all clastic volcanic materials formed by any process of fragmentation, dispersed by any kind of transporting agent, deposited in any environment or mixed in any significant portion with nonvolcanic fragments” (Fisher, 1961). The terms tuff,

lapilli-tuff, lapillistone, and tuff-breccia are nongenetic, granulometric classifications related to the percentage and size of components, and do not imply a pyroclastic origin (Fisher, 1961; Schmid, 1981; White and Houghton, 2006).

Mafic volcanic rocks of the Kangilleq Formation in the central Kangiusap Kuua comprise mafic pillow lavas, scoria-rich breccias, lapillistone, and tuff (Fig. 3). These rocks consist of a typical greenschist-facies mineral assemblage dominated by actinolite (50 vol %), biotite (15 vol %), chlorite (15 vol %), and calcite (14 vol %), with lesser quartz (5 vol %), epidote (1 vol %), and opaque minerals (trace). Stratiform massive to semimassive sulfide (~10 m thick), underlain by a sulfide stringer zone, occurs in outcrop near the top of the ridge and is repeated near the bottom of the valley through an anticlinal fold. The sulfide-rich rocks are hosted by a siliceous hydrothermal breccia, and mafic tuff breccia, at the top of the mafic volcanic sequence. The massive sulfide is capped by a 1- to 3-m-thick chert layer.

Pillow basalt (B_P) and pillow breccia (B_{Bx})

The pillow basalt flows are dark green and weather to a red-brown color, aphyric and amygdaloidal (5–15%, 1- to 10-mm, quartz-filled amygdules). Pillow structures range in size from 20 to 50 cm and are flattened (~1/4) parallel to flow tops. Drainage cavities are common and filled with fine-grained quartz and iron carbonate (Fig. 4A). Individual flows are 10 to 15 m thick with pillows decreasing in size toward the tops of lava flows, which are marked by a gradational change from intact small pillows to pillow breccia (flow-top breccia) over <1 m, indicating younging to the east (Fig. 4B). Flow-top breccias are 0.5 to 1.5 m thick.

Tuff breccia (T_{Bx})

Tuff breccias dominate the top of the volcanic stratigraphy on the west side of the valley, forming individual beds ranging from 2 to 10 m thick and from matrix to block supported. Beds are massive to crudely bedded with normal grading common (Fig. 4C). Graded bedding indicates younging to the west near the top of the west side of the valley, with a reversal to east younging near the pillow basalt flows to the east (Figs. 2, 3). The unit consists of round, aphyric, amygdaloidal to scoriaceous basalt blocks (6–50 cm, 25–75%) in a matrix of fine-grained mafic tuff.

Lapillistone (L_P)

Mafic lapillistone beds are massive, 2 to 3 m thick, and occur between mafic tuff breccia beds where they have sharp upper and lower contacts. Beds consist of >75% subround, mafic lapilli (2–20 mm) within a mafic tuff matrix. Round blocks (<5%) of aphyric, amygdaloidal basalt occur in each tuff bed.

Tuff (T)

Mafic tuff beds are massive to planar laminated and commonly display normal grading. Individual beds vary in thickness from 10 to 40 cm with overall “packages” of tuff beds ranging from 1 to 6 m (Fig. 4D). Scour structures are common, as are round, basalt blocks, which can account for up to 15 vol % of an individual bed. Upper and lower contacts of the tuff units are sharp with tuff breccia units.

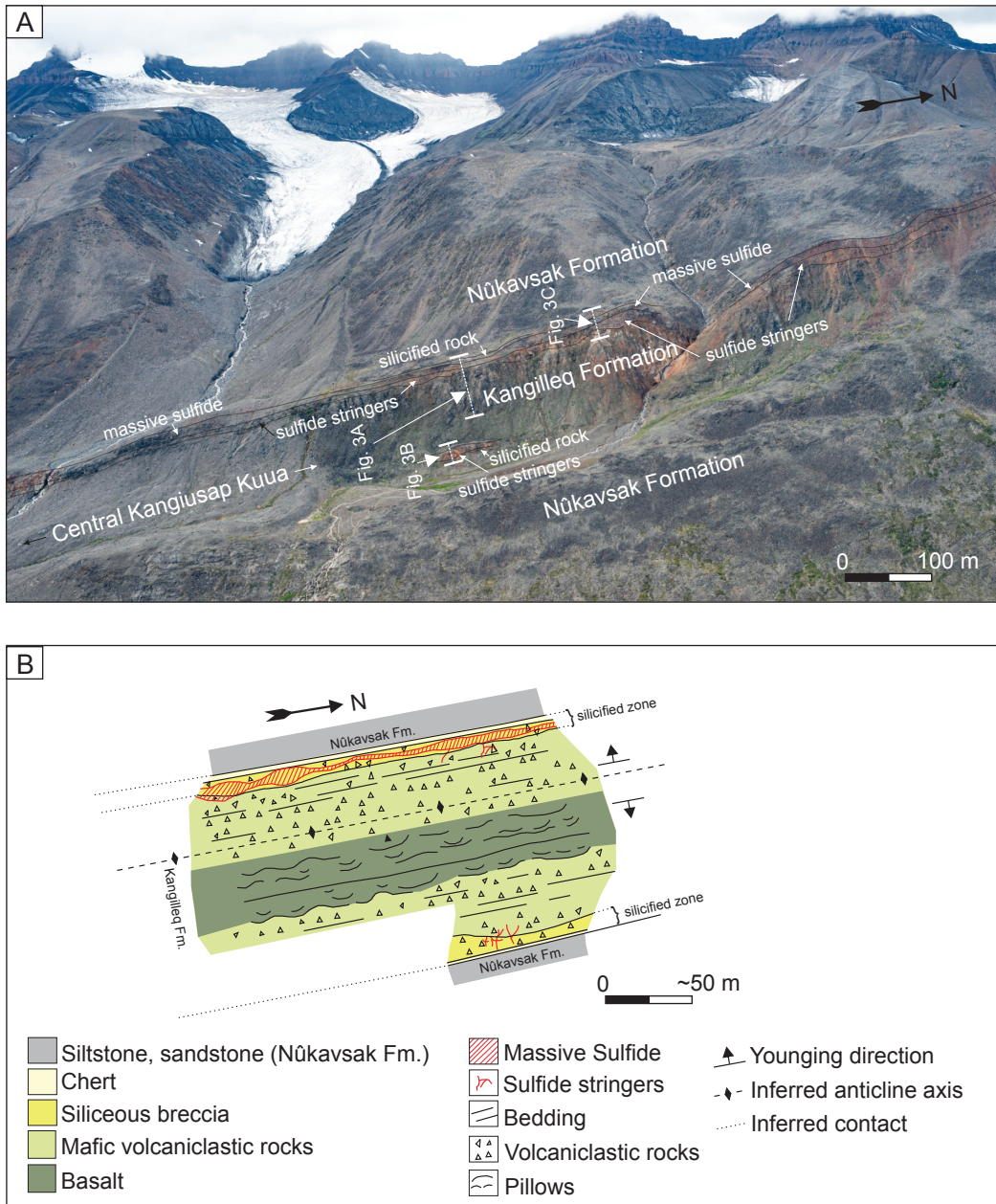


Fig. 2. A. Oblique aerial photo (looking west) of the Kangilleq Formation and contained sulfide mineralization and the bounding Nûkavsak Formation. B. Sketch map (scale approximate), based on field observations, depicting main distribution of lithofacies and mineralization that delineates anticline; closure to the north is based on previous mapping (Escher, 1980). Locations of sections in Figure 3 shown by dashed white lines.

Siliceous breccia (with sulfide stringers; H_{Bx})

An ~3-m-thick siliceous breccia occurs at the top of the mafic volcanic strata. It crops out at the top of the valley where it hosts the massive to stringer sulfide mineralization and in the bottom of the valley where it hosts stringer sulfide mineralization. The unit has a chicken coop wire-like texture with pale yellow, angular fragments (1–20 mm) of very fine grained quartz separated by thin (mm-scale) dark gray zones of quartz, pyrite, and pyrrhotite (Fig. 4E). Its contact with the underlying mafic volcanoclastic rocks is gradational over several meters; the upper contact is not exposed.

Massive to stringer sulfide mineralization (M_S)

The massive sulfide mineralization is ~10 m thick with an underlying semimassive to disseminated sulfide and stringer zone that is <10 m thick. The massive sulfide mineralization is stratiform, occurring within the hydrothermal breccia that caps the mafic volcanic strata, as well as within mafic breccias just below the hydrothermal breccia. The massive sulfide crops out at the top of the ridge where it is relatively continuous over a strike length of ~2,000 m (Fig. 4F). The massive to semimassive sulfide is weathered at surface and consists predominantly of coarse, euhedral pyrite and euhedral to sub-

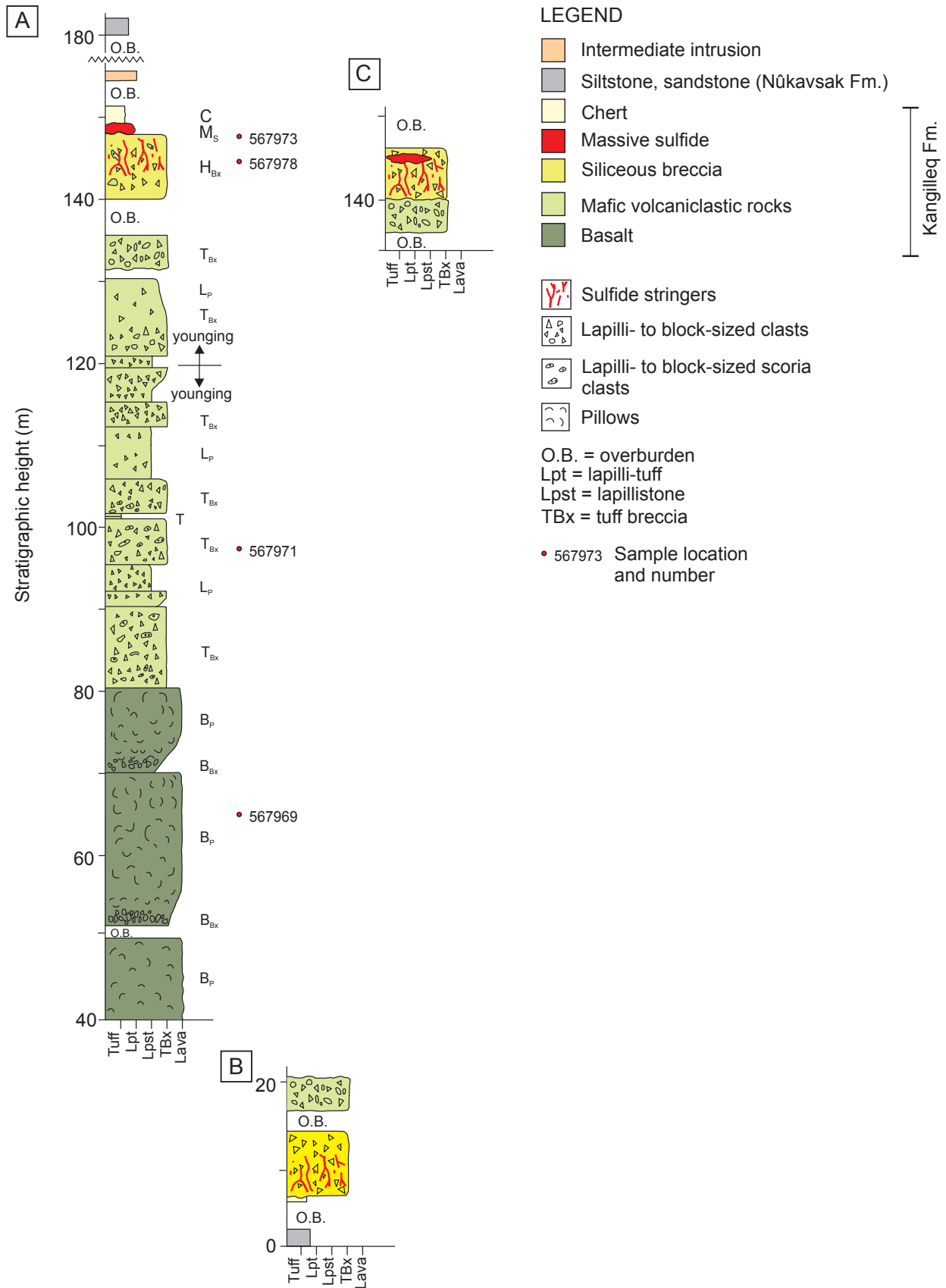


Fig. 3. Stratigraphic columns from south (A) to north (C; see Fig. 2 for locations), showing distribution of lithofacies and sulfide mineralization as well as reversal in younging direction. Lithofacies abbreviations match those in text.

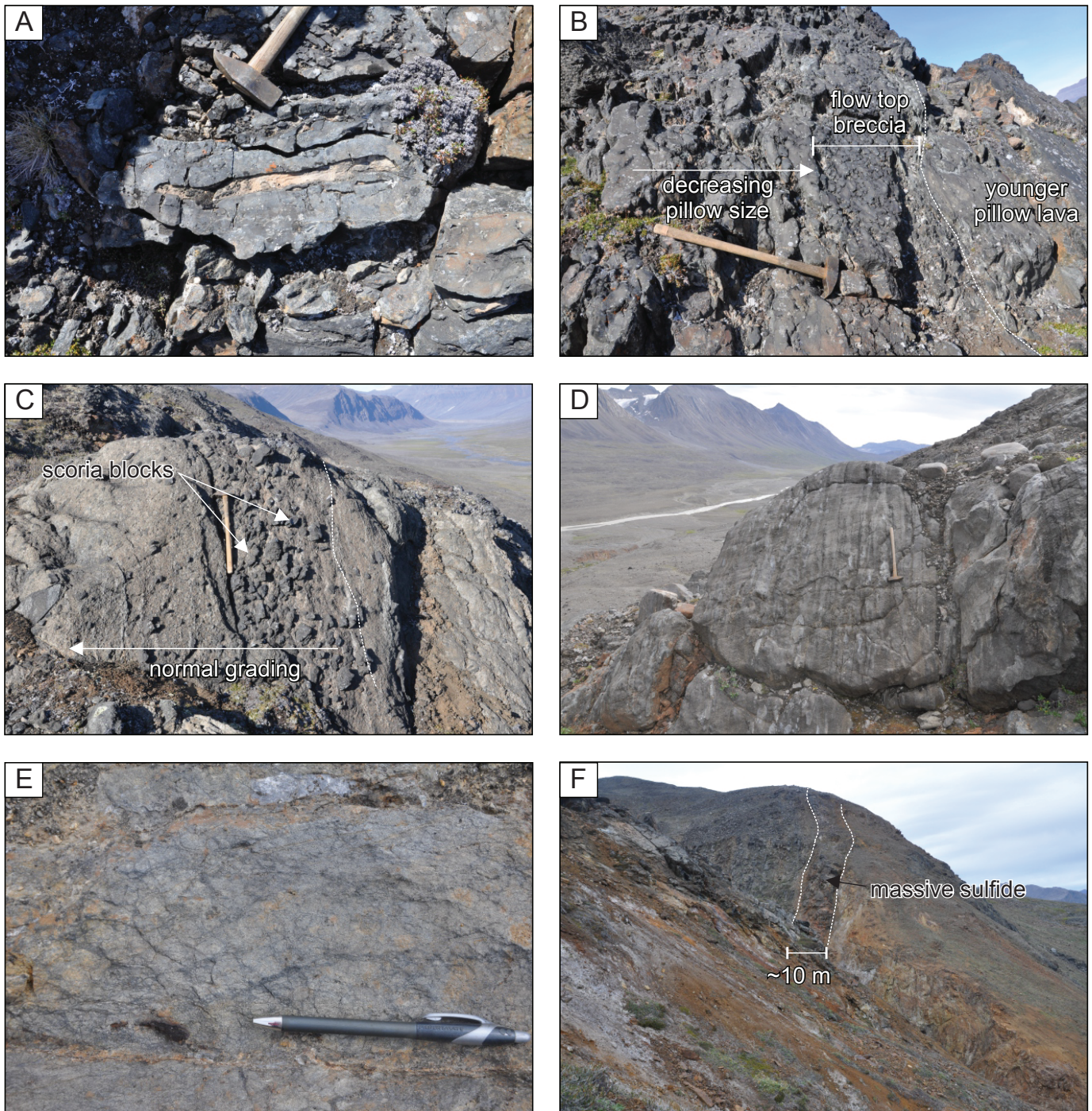


Fig. 4. Field photos of volcanic strata and massive sulfide mineralization in central Kangiusap Kuua. A. Basalt pillow with drainage cavity filled with Fe carbonate. B. Pillow basalt showing gradational transition from larger to smaller pillows to pillow breccia, indicating younging to the right (east). Dashed white line marks contact with base of overlying pillowed flow (far right). C. Bed that grades from block-rich (scoriaeous tuff breccia) to block-poor (tuff), indicating younging to left (west). D. Planar-laminated mafic tuff with rare basalt blocks. E. Silicified and chloritized breccia that hosts the sulfide mineralization. F. Conformable massive sulfide as viewed along strike across a coulee.

hedral pyrrhotite with trace amounts of sphalerite and chalcopyrite that occur as interstitial, anhedral grains ($\sim 100\ \mu\text{m}$) in a fine-grained quartz and graphite matrix (Fig. 5A-C). Secondary hematite forms fracture fillings within pyrrhotite and as veinlets cutting earlier, coarse pyrite and pyrrhotite (Fig. 5C).

The semimassive sulfide zone transitions down stratigraphy (where it is hosted by mafic volcanoclastic rocks) to a disseminated sulfide zone dominated by fine-grained pyrrhotite and pyrite. This zone of disseminated sulfide also hosts the sulfide stringer zone, which consists of 1- to 90-cm-wide pyrrhotite-

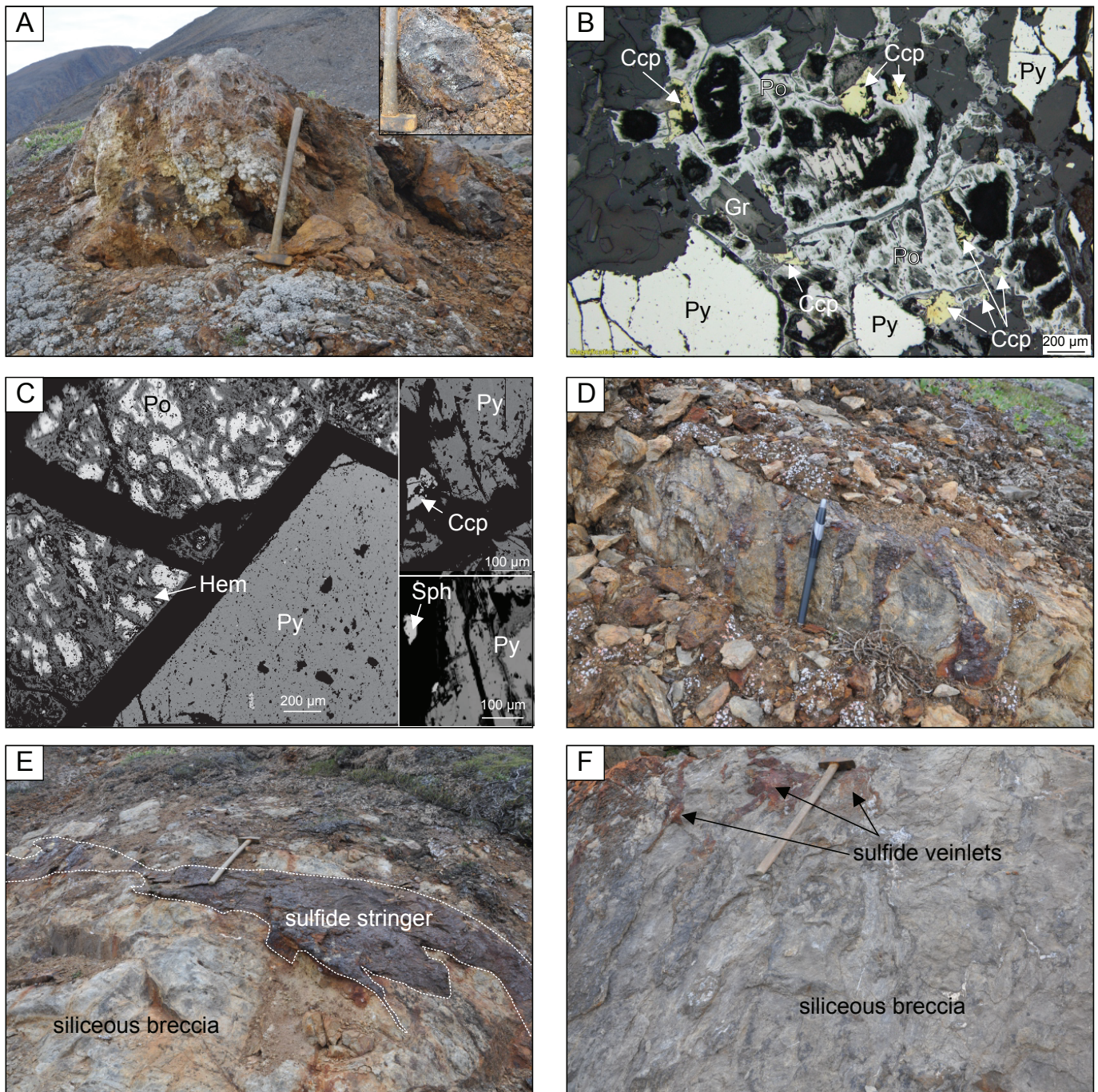


Fig. 5. Field photos and photomicrographs of sulfide mineralization in central Kangiusap Kuua. A. Massive sulfide. Inset photo shows less-weathered coarse pyrite. B. Reflected-light photomicrograph of coarse pyrite and pyrrhotite and fine-grained chalcopyrite within massive sulfide zone (Ccp = chalcopyrite, Gr = graphite, Hem = hematite, Po = pyrrhotite, Py = pyrite, Sph = sphalerite). C. Backscattered electron image of coarse euhedral pyrite and pyrrhotite (partially replaced by secondary hematite along fractures) in massive sulfide. Inset photos show chalcopyrite and sphalerite interstitial to iron sulfides. D. Sulfide stringers in strongly silicified rock with rare basalt clasts. E. Sulfide stringer in siliceous breccia. F. Sulfide stringers or veinlets in strongly siliceous breccia at bottom of the valley.

pyrite stringers with trace chalcopyrite (Fig. 5D, E). A disconformable zone of chlorite alteration occurs in the upper ~20 m of the volcanic succession proximal to the sulfide stringer zone. A stringer sulfide zone is also present in a siliceous breccia and in mafic volcanic rocks near the bottom of the valley (Fig. 5F).

Chert (C)

Overlying the massive sulfide-hosting hydrothermal breccia is a very fine grained, massive, conformable, chert layer (~1–3 m) consisting entirely of recrystallized quartz with trace opaque minerals. The contact with the underlying massive

sulfide and the overlying Nûkavsak Formation is covered by 1 to 5 m of overburden.

Geochemistry

Whole-rock geochemistry

Whole-rock major and trace element geochemical analyses were done on a sample of pillow basalt, a basalt clast from the tuff breccia and two of the siliceous breccia host rocks for the sulfide mineralization (Table 1).

Previous work defined rocks of the Kangilleq Formation as alkaline (Rosa et al., 2017, 2018). However, mafic volcanic rocks of the central Kangiusap Kuua area have Zr/Ti and Nb/Y ratios typical of subalkaline basalt (Fig. 6A). Th-Zr-Nb systematics indicate characteristics similar to those of modern midocean ridge basalt (MORB; Fig. 6B) with Ti/V ratios like modern MOR or back-arc basin (BAB) basalts (Fig. 6C). Niobium/Yb (2.41–3.07), Th/Yb (0.15–0.24), Zr/Yb (44.0–45.9), Th/Nb (0.05–0.10), and La/Sm (1.1–1.9) ratios are similar to those for modern, enriched (E)-MORB. The basalt at central Kangiusap Kuua has relatively flat REE patterns with only a slight enrichment in the light REEs (Fig. 6D, E). A small positive Eu anomaly in one sample of a weakly altered basalt most likely reflects high-temperature hydrothermal alteration under reducing conditions. A least altered sample of pillow basalt (567569) yields an $\epsilon_{Nd(1.9 Ga)}$ value of 3.8.

Sulfide assay geochemistry

Assay results from five massive to semimassive sulfide samples support field and petrographic observations that the mineralization consists predominantly of iron sulfide minerals and is hosted by a siliceous hydrothermal breccia and strongly chlorite and quartz altered basalt breccia. Contents of total Fe range from 34 to 51 wt % and S from 23 to 34 wt %, with uniformly low Cu values from 0.01 to 0.03 wt %, Zn values of <0.02 wt %, and Ni values of 0.01 to 0.14 wt %.

Discussion

Interpretation of lithofacies

The lithofacies, bedforms, and internal stratigraphy of the Kangilleq Formation, in the central Kangiusap Kuua area, suggest the units are the product of subaqueous volcanic eruptions that record sea-floor mass wasting events along fault scarps, likely related to rifting, and that indicate a vent distal environment. The absence of hummocky cross stratification, ripple marks, or accretionary lapilli argues against the mafic volcanoclastic rocks of the central Kangiusap Kuua having been deposited above storm wave base.

The closely packed, small pillows in the central Kangiusap Kuua area resemble those described by Dimroth et al. (1978) as developing during the waning stages of a subaqueous eruption when flow velocity and temperature have decreased, but it could also mean that eruption rates were inherently low or that these pillows represent a vent distal environment. The thickness of individual beds of tuff breccia units, as well as crude layering and the rounding of clasts within units, also indicates a more vent distal environment.

In addition to determining vent distal versus vent proximal deposition, the type and distribution of volcanic lithofacies can

aid in the interpretation of the location of synvolcanic faults, which commonly define the limits of thick permeable volcanoclastic deposits and are critical features in areas of VMS mineralization as they act as highly focused fluid pathways during VMS formation (e.g., Gibson et al., 1999; Stix et al., 2003). The graded beds and scour structures of the mafic tuff and lapillistone indicate deposition from high-density turbidity currents, generated along fault scarps, and the planar laminated beds indicate a decrease in energy leading to suspension deposition from the water column (Lowe, 1982; Mueller et al., 2000).

Based on bedforms and clast concentrations, the tuff breccia units in the central Kangiusap Kuua area are interpreted to have been deposited by both high-concentration mass flows (e.g., clast-supported tuff breccia beds with massive bedforms and scour structures) and lower concentration mass flows (e.g., matrix-supported tuff breccia beds; Mueller et al., 2000). Blocks of aphyric and scoriaceous basalt were derived from the substrate during emplacement and entrained in the high-energy mass flow. The block-size clasts and monolithic nature of these breccias suggest that they represent a syn-eruptive, resedimented deposit possibly derived by collapse along nearby fault scarps (Fig. 7). The sharp, conformable contacts separating these units imply that each represents a distinct debris flow event. The discontinuous nature of volcanic lithofacies along strike (e.g., variations in lithofacies on west and east limbs of the anticline) is also consistent with the presence of synvolcanic faulting. Synvolcanic faults would have not only controlled lithofacies type (e.g., coarse breccias) and their distribution, but also likely acted as pathways for hydrothermal fluids to circulate and ascend. The cross-stratal permeability, provided by synvolcanic faults, coupled with these faults facilitating the accumulation (i.e., within a graben defined by synvolcanic faults) of thick packages of porous, water-saturated volcanic debris on the sea floor would have aided in the precipitation of sulfide minerals within mafic volcanoclastic deposits on the sea floor (i.e., replacement-style massive and stringer sulfide mineralization). The siliceous breccia at the top of the basaltic sequence could represent strongly silicified basalt breccias, but given its mineralogy and chemistry, which is >95% quartz, it is more likely that this unit represents a primary hydrothermal breccia that would have served as a thermal and in part mechanical seal to the hydrothermal system, as inferred for the formation of such breccias in many ancient VMS deposits, and facilitated the seafloor replacement of permeable mafic volcanoclastic rocks (Fig. 7; Gibson and Kerr, 1993; Franklin et al., 2005). The presence of a 1- to 3-m-thick chert layer at the top of the sequence likely represents what would have been a seawater-saturated siliceous ooze, which could have also aided in seafloor replacement-style mineralization that has been observed in other VMS deposits (e.g., Wolverine and Duck Pond, Canada; Piercey, 2015).

Volcanic and tectonic setting

The Karrat Group has been attributed to deposition during the evolution from a restricted shallow-marine (Qaarsukasak, Mârmorilik, and Kangilleq Formations), passive margin sequence to a foreland basin succession in response to the Thelon orogeny (Nûkavsak Formation; Sanborn-Barrie et al., 2017). However, the geologic characteristics of the Kangilleq

Table 1. Major and Trace Element Whole-Rock Geochemistry for Selected Samples from the Kangilleq Formation in the Central Kangiasuap Kuua

Sample	567969	567971	567973	567978
Description	Pillow basalt	Basalt clast from tuff breccia	Silicified and chloritized host rock to massive sulfide	Silicified host to sulfide stringer
Latitude	71.875676N	71.875914N	71.875864N	71.880162N
Longitude	53.991332W	53.993484W	53.994261W	53.997624W
SiO ₂ (wt %)	47.88	46.92	96.24	90.48
Al ₂ O ₃	12.16	15.46	0.19	0.23
Fe ₂ O ₃ (total)	12.73	8.52	1.62	5.83
MnO	0.188	0.066	0.009	0.023
MgO	10.82	10.60	0.05	0.04
CaO	10.54	13.50	0.03	0.07
Na ₂ O	2.41	1.48	0.03	0.02
K ₂ O	0.19	0.55	0.03	0.04
TiO ₂	1.343	1.525	0.015	0.014
P ₂ O ₅	0.08	0.16	<0.01	<0.01
LOI	0.68	1.85	1.38	3.00
Total	99.03	100.6	99.6	99.75
Sc (ppm)	43	48	<1	<1
Be	<1	1	<1	<1
V	330	356	54	92
Cr	670	1360	<20	40
Co	62	34	<1	9
Ni	200	100	<20	90
Cu	40	<10	20	10
Zn	80	90	<30	<30
Ga	15	14	<1	<1
Ge	1.5	1.5	0.6	<0.5
As	<5	<5	6	37
Rb	<1	9	<1	<1
Sr	161	286	<2	<2
Y	16.8	18.1	0.7	0.8
Zr	66	78	4	8
Nb	4.6	4.1	<0.2	0.3
Mo	<2	<2	6	29
Ag	<0.5	<0.5	<0.5	<0.5
In	<0.1	<0.1	<0.1	<0.1
Sn	<1	1	<1	<1
Sb	<0.2	<0.2	0.4	0.4
Cs	0.1	1.6	<0.1	<0.1
Ba	40	147	12	66
La	3.25	5.53	0.65	0.63
Ce	9.53	15.5	0.83	0.85
Pr	1.59	2.39	0.12	0.16
Nd	9.67	10.8	0.45	0.52
Sm	3.03	2.89	0.07	0.11
Eu	0.930	1.570	0.034	0.022
Gd	3.30	3.53	0.11	0.12
Tb	0.57	0.59	0.02	0.02
Dy	3.42	3.64	0.10	0.11
Ho	0.67	0.70	0.02	0.02
Er	1.74	2.02	0.05	0.06
Tm	0.249	0.266	0.007	0.009
Yb	1.50	1.70	0.04	0.06
Lu	0.221	0.252	0.004	0.010
Hf	0.9	1.1	<0.1	<0.1
Ta	0.3	0.35	<0.01	<0.01
W	<0.5	5	<0.5	1.3
Tl	<0.05	<0.05	<0.05	<0.05
Pb	<5	<5	9	9
Bi	<0.1	<0.1	<0.1	<0.1
Th	0.23	0.40	0.21	0.38
U	0.03	1.69	4.06	8.49
Eu _{ch}	16.0	27.1	0.6	0.4

Note: Eu-normalized chondrite (ch) values from Sun and McDonough (1989)

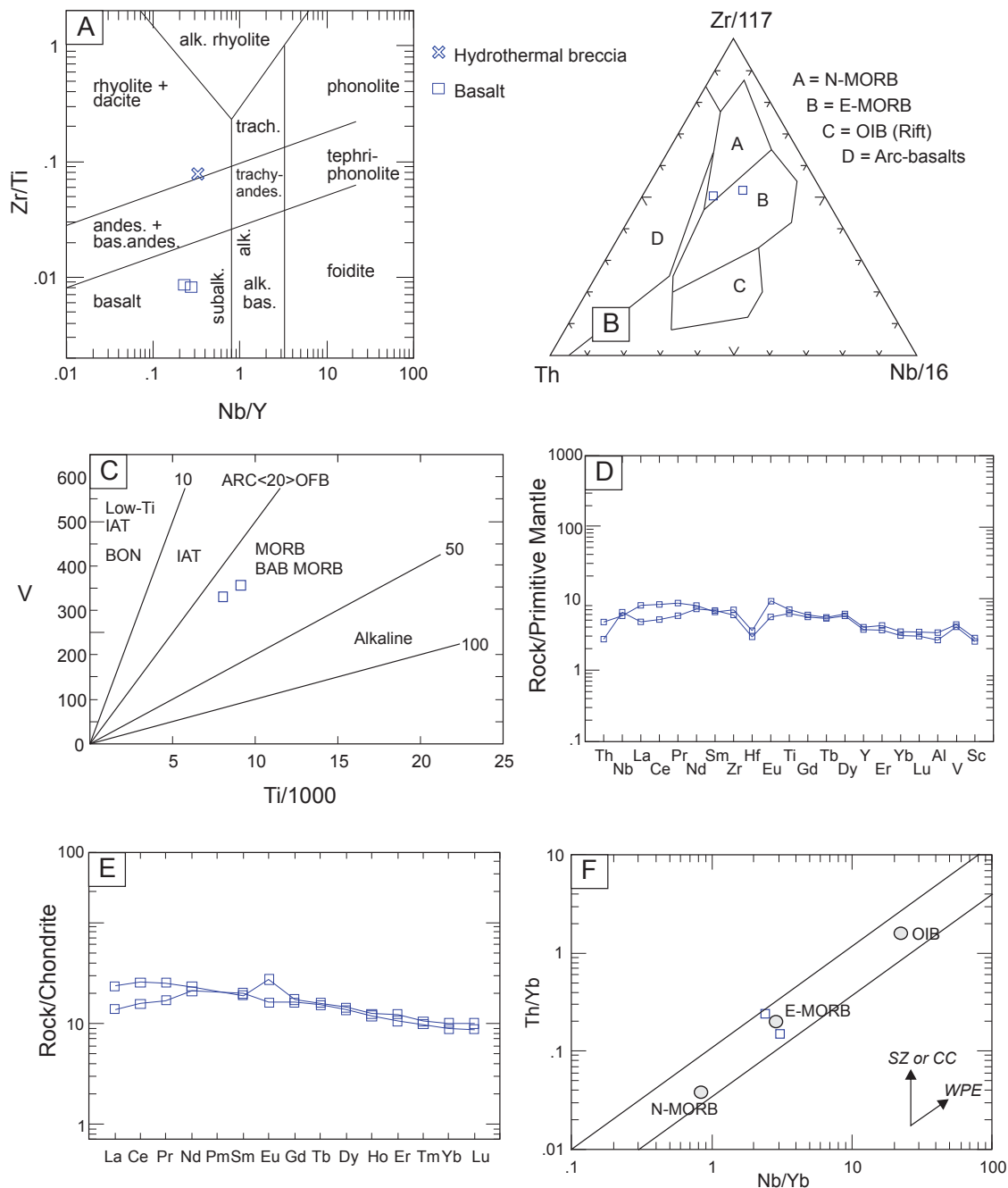


Fig. 6. Whole-rock geochemistry diagrams for volcanic rocks of the Kangilleq Formation in central Kangiusap Kuua. A. Classification diagram for volcanic rocks (Pearce, 1996). B. Th-Zr-Nb tectonomagmatic discrimination diagram (Wood, 1980). C. Ti vs. V tectonomagmatic discrimination diagram (Shervais, 1982). BABB = back-arc basin basalt, BON = boninite, IAT = island-arc tholeiitic basalt, MORB = mid-ocean ridge basalt, OFB = ocean-floor basalt. D. Primitive mantle-normalized trace element plot. Primitive mantle values from Sun and McDonough (1989). E. Chondrite-normalized rare earth element plot. Chondrite values from Sun and McDonough (1989). F. Th/Yb vs. Nb/Yb diagram, illustrating an E-MORB signature, from Pearce (2008). N-MORB, E-MORB, and OIB values from Sun and McDonough (1989).

Formation presented here indicate that it records subaqueous mafic volcanism and synvolcanic massive sulfide mineralization in an extensional setting. Mafic volcanic rocks in the central Kangiusap Kuua are subalkaline with Zr/Y ratios (4–6) that indicate transitional to tholeiitic geochemical affinities. In Nb/Yb versus Th/Yb space, samples lie within the E-MORB field, suggesting derivation from an enriched mantle source

(Fig. 6F). Niobium/Th and Nb/Zr values are also consistent with those of modern E-MORB (Sun and McDonough, 1989). However, considering the Nd isotope data, which yield an initial ϵ_{Nd} value very close to the Paleoproterozoic depleted mantle (DePaolo, 1981), we interpret the E-MORB signature to represent a minor subduction zone input, as would be found in a back-arc basin. Thus, our interpretation is that this

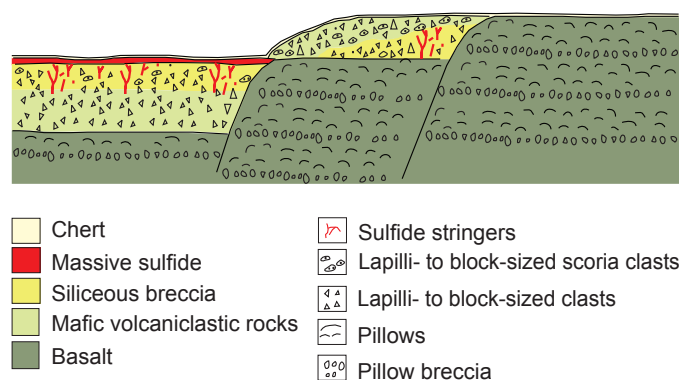


Fig. 7. Schematic cross section of volcanic environment during sulfide formation. Subseafloor replacement of mafic volcanoclastic rocks by massive sulfide and sulfide stringers, with cross-stratal fluid flow aided by synvolcanic growth faults. Normal faulting also created basins into which volcanoclastic material was deposited, likely by mass debris flows generated along fault scarps.

sequence formed in response to back-arc rifting on a continental margin.

Evidence of VMS-type mineralization

Ancient VMS deposits formed in areas of localized rifting or extension within overall collisional environments, such as continental or island arcs (e.g., Franklin et al., 2005). Synvolcanic faulting in these localized areas of extension results in the formation of basins in which porous volcanoclastic debris accumulates and, consequently, commonly results in local discontinuities in stratigraphy (e.g., Scott et al., 2003; Wright et al., 2003). This combination of wet, porous volcanoclastic deposits on the sea floor, and their spatial association with synvolcanic faults that act as hydrothermal fluid pathways, is critical in the process of subseafloor replacement-style mineralization common in many VMS deposits (e.g., Franklin et al., 2005; Piercey, 2015). The discontinuous nature of volcanic stratigraphy along strike in the central Kangiusap Kuua is shown by changes in lithofacies on either side of the anticlinal fold axis (Figs. 2, 3). Thicknesses of volcanoclastic units, their lack of continuity along strike, and inferred derivation from mass wasting events along fault scarps suggest a rift environment and deposition within a subsidence structure resulting from this rifting. Margins of the basin are therefore interpreted to be synvolcanic, normal faults that may have also acted as hydrothermal fluid pathways, resulting in subseafloor replacement of the permeable volcanoclastic deposits that had accumulated on the sea floor. The presence of a conformable massive to semimassive sulfide lens underlain by a disconformable sulfide stringer, or stockwork zone, hosted within strongly quartz altered hydrothermal breccias and mafic volcanoclastic rocks is strong evidence that the sulfide zone at central Kangiusap Kuua represents VMS-type mineralization. The semiconformable zone of quartz alteration and disconformable zone of chlorite alteration that occur in the upper ~20 m of the volcanic succession, and contain the mineralized zone, are similar to what is found in alteration zones in VMS deposits globally and are further evidence of a hydrothermal VMS system.

VMS deposits are subdivided into five subtypes based largely on the lithostratigraphic sequence in which they are found

(Franklin et al., 2005). Because the host stratigraphic succession in the central Kangiusap Kuua is dominated by metamorphosed mafic volcanic and siliciclastic rocks, the mineralized setting most resembles that of the pelite-mafic VMS subtype (e.g., Besshi, Windy Craggy). This assignment is also consistent with the interpreted tectonic setting for the mafic volcanic rocks of a back-arc rift that developed on a continental margin.

Significance of VMS mineralization in central Kangiusap Kuua

The massive sulfide lens is ~10 m thick in outcrop, and although the lens can be followed over 2 km along strike, it is dominated by pyrite with only subeconomic base metal grades (<0.05 wt % Cu + Zn + Pb). Despite being dominated by subeconomic iron sulfides, this is clearly an extensive system as evidenced by its strike length, thickness, substantive zone of quartz alteration, and the presence of both a hydrothermal breccia and chert cap. The mineralization is associated with volcanogenic debris flows, interpreted to have formed from mass wasting from somewhat vent distal synvolcanic fault scarps. If that is the case, then it is possible that vent proximal mineralization would have a more economically significant mineral assemblage, compared to the distal, iron-rich sulfide mineralization, as is observed in other VMS camps (Goodfellow, 2007; Hollis et al., 2015).

Assignment here of the central Kangiusap Kuua massive sulfide occurrence to the pelite-mafic VMS subtype allows for the first time an ore deposit specific exploration model for the area north of Kangerlussuaq-Upernivik (Fig. 1). This study not only characterizes the central Kangiusap Kuua VMS, but also potentially explains other massive sulfide occurrences in the area and identifies the entire region north of Kangerlussuaq-Upernivik (Fig. 1) as a prospective target for VMS exploration.

Conclusions

A siliceous hydrothermal breccia and mafic volcanoclastic rocks of the Kangilleq Formation at central Kangiusap Kuua host conformable massive to semimassive sulfide underlain by a disconformable sulfide stringer zone. The hydrothermal footprint of this mineralization includes a semiconformable zone of quartz alteration, and a disconformable chlorite alteration zone. The stratigraphic succession (dominated by metamorphosed mafic volcanic and siliciclastic rocks) and sulfide mineral assemblage (dominated by pyrrhotite and pyrite with trace sphalerite and chalcopyrite) indicate that the mineralization fits the pelite-mafic VMS subtype classification and therefore is the first significant documentation of VMS mineralization in Greenland.

Mafic volcanic and volcanoclastic rocks of the Kangilleq Formation in the central Kangiusap Kuua formed in a submarine environment and represent syneruptive, resedimented deposits possibly derived by collapse along nearby fault scarps and deposition by both mass flows and suspension sedimentation. Trace element data indicate that the basalts are subalkaline, are transitional to tholeiitic in nature, and have geochemical attributes similar to E-MORB; Nd isotope data indicate a depleted mantle source. Utilizing the regional and local stratigraphic context of the volcanic rocks, trace element characteristics, Nd isotope value, and presence of a VMS occurrence,

we suggest that eruption, deposition, and mineralization occurred in a back-arc basin on a continental margin.

Acknowledgments

This research was conducted as part of the larger collaborative Karrat Zinc Project of the Geological Survey of Denmark and Greenland (GEUS) and the Ministry of Mineral Resources (MMR), focusing on 1:100,000 mapping and mineral potential evaluation of the Karrat Group. Logistical and financial support was provided by several sources including GEUS, MMR, and an NSERC Discovery Developmental Grant to Y. M. DeWolfe (DDG-2018-00008). The authors offer sincere thanks to John Slack, Neil Rogers, and Associate Editor Stephen Piercey for thorough and thought-provoking reviews that greatly improved this manuscript.

REFERENCES

- Allen, R.L., Weihed, P., and the Global VMS Research Project Team, 2002, Global comparison of volcanic-associated massive sulphide districts: Geological Society of London Special Publication 204, p. 13–37.
- Allen, R.L., Tornos, F., and Peter, J.M., 2011, A thematic issue on the geological setting and genesis of volcanogenic massive sulfide (VMS) deposits: *Mineralium Deposita*, v. 46, p. 429–430, doi.org/10.1007/s00126-011-0368-1.
- Connelly, J.N., Thrane, K., Krawiec, A.W., and Garde, A.A., 2006, Linking the Palaeoproterozoic Nagssugtoqidian and Rinkian orogens through the Disko Bugt region of West Greenland: *Journal of the Geological Society*, v. 163, p. 319–335.
- Daves, P.R., 2006, Explanatory notes to the geological map of Greenland, 1:500 000, Thule, Sheet 5: Geological Survey of Denmark and Greenland Map Series, 2, p. 1–100, https://doi.org/10.34194/geusm.v2.4614.
- DePaolo, D.J., 1981, Neodymium isotopes in the Colorado Front Range and crust-mantle evolution in the Proterozoic: *Nature*, v. 291, p. 193–196.
- Dimroth, E. and Yamagishi, H., 1987, Criteria for the recognition of ancient subaqueous pyroclastic rocks: Report Geological Survey of Hokkaido, v. 58, p. 55–88.
- Dimroth, E., Cousineau, P., Leduc, M., and Sanschagrin, Y., 1978, Structure and organization of Archean subaqueous basalt flows, Rouyn-Noranda area, Quebec, Canada: *Canadian Journal of Earth Sciences*, v. 15, p. 902–918.
- Escher, J.C., comp., 1980, Upernavik Isfjord: Geological map of Greenland: Geological Survey of Greenland, Map sheet no. 4, scale 1:500,000.
- Fisher, R.V., 1961, Proposed classification of volcanoclastic sediments and rocks: *Geological Society of America Bulletin*, v. 72, p. 1395–1408.
- Franklin, J.M., Gibson, H.L., Galley, A.G., and Jonasson, I.R., 2005, Volcanogenic massive sulfide deposits: *Economic Geology 100th Anniversary Volume*, p. 523–560.
- Galley, A.G., Hannington, M.D., and Jonasson, I., 2007, Volcanogenic massive sulphide deposits: Geological Association of Canada, Mineral Deposits Division Special Publication 5, p. 141–161.
- Garde, A.A., and Hollis, J.A., 2010, A buried Palaeoproterozoic spreading ridge in the northern Nagssugtoqidian orogen, West Greenland: *Geological Society of London Special Publication* 338, p. 213–234.
- Garde, A.A., and Pulvertaft, T.C.R., 1976, Age relations of the Precambrian Marmorilik Marble Formation, central West Greenland: *Geological Survey of Greenland Report* 80, p. 49–53.
- Gibson, H.L., and Kerr, D.J., 1993, A comparison of the Horne volcanogenic massive sulfide deposit and intracauldron deposits of the Mine sequence, Noranda, Quebec: *Economic Geology*, v. 88, p. 1419–1442.
- Gibson, H.L., Morton, R.L., and Hudak, G.J., 1999, Submarine volcanic processes, deposits and environments favorable for the location of volcanic-hosted massive sulfide deposits: *Reviews in Economic Geology*, v. 8, p. 13–51.
- Goodfellow, W.D., 2007, Metallogeny of the Bathurst mining camp, northern New Brunswick: Geological Association of Canada, Mineral Deposits Division, Special Publication 5, p. 449–469.
- Guarnieri, P., Partin, C.A., and Rosa, D., 2016, Palaeovalleys at the basal unconformity of the Palaeoproterozoic Karrat Group, West Greenland: *Geological Survey of Denmark and Greenland Bulletin*, v. 35, p. 63–66.
- Guarnieri, P., Baker, N., Rosa, D., and Sørensen, E.V., 2022a, Geological map of Greenland, Maarmorilik 71 V. 2 Syd: Geological Survey of Denmark and Greenland, Copenhagen, scale 1:100,000, https://doi.org/10.22008/FK2/07OYKX.
- 2022b, Geological map of Greenland, Nuugaatsiaq 71 V. 2 Nord: Geological Survey of Denmark and Greenland, Copenhagen scale 1:100,000, https://doi.org/10.22008/FK2/PGSMJH.
- 2022c, Geological map of Greenland, Pannertooq 7 V. 2 Syd: Geological Survey of Denmark and Greenland, Copenhagen, scale 1:100,000, https://doi.org/10.22008/FK2/IBHIZL.
- Hannington, M.D., 2014, Volcanogenic massive sulfide deposits: *Treatise on Geochemistry*, 2nd ed., p. 463–488.
- Henderson, G., and Pulvertaft, T.C.R., 1967, The stratigraphy and structures of the Precambrian rocks of the Umanak area, West Greenland: *Meddelelser fra Dansk Geologisk Forening*, v. 17, p. 1–20.
- 1987, Geological map of Greenland, Marmorilik 71 V.2 Syd, Nûgâtsiaq 71 V.2 Nord, Pangnertôq 72 V.2 Syd: Geological Survey of Greenland, scale 1:100,000, 72 p.
- Hollis, S.P., Cooper, M.R., Herrington, R.J., Roberts, S., Earls, G., Verbeeten, A., Piercey, S.J., and Archibald, S.M., 2015, Distribution, mineralogy and geochemistry of silica-iron exhalites and related rocks from the Tyrone Igneous Complex: Implications for VMS mineralization in Northern Ireland: *Journal of Geochemical Exploration*, v. 159, p. 148–168.
- Kolb, J., Keiding, J.K., Steenfelt, A., Secher, K., Keulen, N., Rosa, D., and Stensgaard, B.M., 2016, Metallogeny of Greenland: *Ore Geology Reviews*, v. 78, p. 493–555.
- Lowe, D.R., 1982, Sediment gravity flows: II. Depositional models with special reference to the deposits of high-density turbidity currents: *Journal of Sedimentary Petrology*, v. 52, p. 279–297.
- Lydon, J.W., 1984, Ore deposit models. 8. Volcanogenic massive sulphide deposits. Pt. 1: A descriptive model: *Geoscience Canada*, v. 11, p. 195–202.
- Mueller, W.U., Garge, A.A., and Stendal, H., 2000, Shallow-water, eruption-fed, mafic pyroclastic deposits along a Paleoproterozoic coastline: Kangerluluk volcano-sedimentary sequence, southeast Greenland: *Precambrian Research*, v. 101, p. 163–192.
- Ohmoto, H., 1996, Formation of volcanogenic massive sulfide deposits: The Kuroko perspective: *Ore Geology Reviews*, v. 10, p. 135–177.
- Østergaard, C., Garde, A.A., Nygaard, J., Blomsterberg, J., Nielsen, B.M., Stendal, H., and Thomas, C.W., 2002, The Precambrian supracrustal rocks in Natanaq (Lersletten) and Ikamiut areas, central West Greenland: *Geology of Greenland Survey Bulletin* 191, p. 24–32.
- Pearce, J.A., 1996, A user's guide to basalt discrimination diagrams: Geological Association of Canada Short Course Notes, v. 12, p. 79–113.
- 2008, Geochemical fingerprinting of oceanic basalts with applications to ophiolite classification and the search for Archean oceanic crust: *Lithos*, v. 100, p. 14–48.
- Piercey, S.J., 2015, A semipermeable interface model for the genesis of sub-seafloor replacement-type volcanogenic massive sulfide (VMS) deposits: *Economic Geology*, v. 110, p. 1655–1660.
- Pollock, J.C., Sylvester, P.J. and Barr, S.M., 2015, Lu-Hf zircon and Sm-Nd whole-rock isotope constraints on the extent of juvenile arc crust in Avalonia: Examples from Newfoundland and Nova Scotia, Canada: *Canadian Journal of Earth Sciences*, v. 52, p. 161–181.
- Rosa, D., DeWolfe, Y.M., Guarnieri, P., Kolb, J., Laflamme, C., Partin, C.A., Salehi, S., Sørensen, E., Thaarup, S., Thrane, K., and Zimmermann, R., 2017, Architecture and mineral potential of the Paleoproterozoic Karrat Group, West Greenland—results of the 2016 season: *Danmarks og Grønlands Geologiske Undersøgelse Rapport* 5, 112 p.
- Rosa, D., Bernstein, S., DeWolfe, Y.M., Dziggel, A., Grocott, J., Guarnieri, P., Kolb, J., Partin, C.A., Sørensen, E., and Zimmermann, R., 2018, Architecture and mineral potential of the Paleoproterozoic Karrat Group, West Greenland—results of the 2017 season: *Danmarks og Grønlands Geologiske Undersøgelse Rapport* 23, 102 p.
- Sanborn-Barrie, M., Thrane, K., Wodicka, N., and Rayner, N., 2017, The Laurentia-West Greenland connection at 1.9 Ga: New insights from the Rinkian fold belt: *Gondwana Research*, v. 51, p. 289–309.
- Schmid, H.-U., 1981, Descriptive nomenclature and classification of pyroclastic deposits and fragments: Recommendations of the IUGS Subcommittee on the systematics of igneous rocks: *Geology*, v. 9, p. 41–43.
- Scott, C.R., Richard, D., and Fowler, A.D., 2003, An Archean submarine pyroclastic flow due to submarine dome collapse: The Hurd deposit, Harker Town-ship, Ontario, Canada: *American Geophysical Union, Geophysical Monograph Series*, v. 140, p. 317–327.

- Shervais, J.W., 1982, Ti-V plots and the petrogenesis of modern and ophiolitic lavas: *Earth and Planetary Science Letters*, v. 59, p. 101–118.
- Stix, J., Kennedy, B., Hannington, M., Gibson, H., Fiske, R., Mueller, W., and Franklin, J., 2003, Caldera-forming processes and the origin of submarine volcanogenic massive sulphide deposits: *Geology*, v. 31, p. 375–378.
- St-Onge, M.R., van Gool, J.A.M., Garde, A.A., and Scott, D.J., 2009, Correlation of Archaean and Palaeoproterozoic units between northeastern Canada and western Greenland: Constraining the pre-collisional upper plate accretionary history of the Trans-Hudson orogeny: *Geological Society of London Special Publication* 318, p. 193–235.
- Sun, S.-s., and McDonough, W.F., 1989, Chemical and isotopic systematics of oceanic basalts: Implications for mantle composition and processes: *Geological Society of London Special Publication* 42, p. 313–345.
- Thrane, K., 2021, The oldest part of the Rae craton identified in western Greenland: *Precambrian Research*, v. 357, 106139, <https://doi.org/10.1016/j.precamres.2021.106139>.
- White, J.D.L., and Houghton, B.F., 2006, Primary volcanoclastic rocks: *Geology*, v. 34, p. 677–680.
- Wood, D.A., 1980, The application of a ThHfTa diagram to problems of tectonomagmatic classification and to establishing the nature of crustal contamination of basaltic lavas of the British Tertiary Volcanic Province: *Earth and Planetary Science Letters*, v. 5, p. 11–30.
- Wright, I.C., Gamble, J.A., and Shane, P.A., 2003, Submarine silicic volcanism of the Healy caldera, southern Kermadec arc (SW Pacific): I. Volcanology and eruption mechanisms: *Bulletin of Volcanology*, v. 65, p. 15–29.

Michelle DeWolfe is a professor of volcanology and igneous petrology at Mount Royal University in Calgary, Alberta, Canada. She attained her Ph.D. in mineral deposits and Precambrian geology from Laurentian University in 2009. Prior to that she worked in mineral exploration for Falconbridge Ltd. (now Glencore PLC) and FNX Mining Ltd. (now KGHM Polska Miedz S.A.). Her current research is focused on VMS deposits of the Slave craton, Trans Hudson orogen, West Greenland, and the northern Appalachians, as well as sea-floor massive sulfide deposits of the southern Indian Ocean.



